The Response of a Nuclear Power Plant to Near-Field Moderate Magnitude Earthquakes

R.P. Kennedy, S.A. Short

Structural Mechanics Associates, 4740 Von Karman, Newport Beach, California 92660, U.S.A.

N.M. Newmark

Nathan M. Newmark Consulting Engineering Services, Urbana, Illinois, U.S.A.

The ground motion input for seismic evaluation and design of nuclear power facilities is specified by broad frequency content design response spectrum anchored to peak ground acceleration. Since 1970, several low-to-moderate magnitude, near-field earthquake records have shown very high peak ground accelerations and elastic response spectra. These peak accelerations and response spectra greatly exceed the SSE accelerations and design spectra used for nuclear power plants in low-to-moderate seismicity regions. The question is whether such exceedance would result in damage? Observations of the behavior of structures subjected to such earthquakes indicate that, although very large peak accelerations have been recorded, there has been only very minor damage in the vicinity of the recording sites. Examples of this behavior include the 1971 Pacoima Dam earthquake record, the 1966 Parkfield earthquake, the 1972 Ancona earthquakes, and the 1972 Melendy Ranch Barn earthquake record which produced peak accelerations of between 0.5 and 1.2g but very little damage.

The purpose of this study was to investigate the effect of high acceleration, low magnitude, near-field earthquake motion on a typical low seismic zone nuclear power plant. Linear and nonlinear seismic analyses were performed on a PWR reactor building subjected to the 0.5g Melendy Ranch Barn motion recorded in the near-field of the 4.7 magnitude Bear Valley Earthquake. This plant was designed for a broad frequency content response spectrum anchored to an SSE acceleration of 0.2g. At the fundamental frequencies of the containment internal structures, the Melendy Ranch Barn response spectrum exceeded the design spectrum by a factor of 2.5. Linear-elastic analysis indicated the base mat uplift resisting capacity was exceeded by a factor of 3.8, the concrete cracking shear capacity of the lower shear walls of the internal structure were exceeded by a factor of 2.3 with the ultimate shear capacity being exceeded at one level; the bond-slip moment was exceeded by a factor of 4.4 at the intersection of the internal structure and base mat; no flexural yielding of the internal structure was predicted; and no nonlinear response of the containment building wall was predicted. Nonlinear response analyses incorporated nonlinear soil-structure interaction effects due to base mat uplift, and stiffness degrading nonlinear shear stiffness and bond-slip for the internal concrete structures. Very conservative stiffness degrading properties were used in order to investigate the possibility of progressive failure due to cyclic degradation of the concrete stiffnesses. This paper describes the development of the nonlinear properties used.

The nonlinear analysis indicates that the base mat uplift height is small (2 mm). Nonlinear story displacements occurred only in the lower portion of the internal structure and were only 3.3 times the displacement at which shear cracking initiated. Despite the assumption of highly degrading concrete stiffnesses, only a single, strong nonlinear response cycle occurred and subsequent response was pseudo-elastic with degraded stiffness. The energy content of the Melendy Ranch Barn record is insufficient to lead to progressive failure. Floor response spectra from the nonlinear analysis were less than or equal to the linear computed floor spectra at all frequencies.

The conclusion is that a 0.5g near-field acceleration time history from a low magnitude earthquake is not damaging to a nuclear power plant structure designed for a broad frequency content response spectrum anchored to an SSE acceleration of 0.2g.

1. Introduction

The majority of the eastern half of the United States and most of Europe are characterized as low-to-moderate seismicity regions with maximum Modified Mercalli Intensities of VIII or less. Within such regions, modern nuclear power plants are typically being designed for a broad frequency content safe-shutdown-earthquake (SSE) response spectrum anchored to a zero period acceleration of about 0.2g. However, such plants might be subjected to much higher ground acceleration and response spectra resulting from a low magnitude, near-field earthquake such as the 1972 Melendy Ranch Barn record which was recorded in the near-field of the magnitude 4.7 Bear Valley earthquake. Figure 1 presents the response spectrum obtained when this recording is normalized to a peak ground acceleration of 0.5g (the actual maximum acceleration essentially equaled 0.5g). This recording is considered typical of records obtained in the near-field from earthquakes with magnitudes less than 5.5. It is characterized by a high peak acceleration, a narrow frequency range for amplified spectral acceleration (4 to 12 Hz), minimal energy content below about 2 Hz, and a very short strong motion duration of about 1.2 seconds. For frequencies of 4.5 Hz and greater, this spectrum exceeds a typical 0.2g SSE design spectrum by factors of 2.5 or greater. The question is whether such ground motion could be damaging to a typical nuclear plant designed for low-to-moderate seismic zones.

This paper investigates the performance of a typical PWR reactor building subjected to the Melendy Ranch Barn record. This study is conservative because it ignores potential mitigating effects such as reduction in ground motion levels with embedment depth, and base mat size and traveling wave effects. The study considers nonlinear soil-structure interaction due to base mat uplift, nonlinear shear and flexural deformation of concrete shear walls, and nonlinear rotation at the intersection of walls with the base mat due to bond-slip.

2. Model Description and Method of Analysis

The typical PWR reactor building considered consists of a prestressed concrete cylindrical external building and roof dome and a reinforced concrete internal structure on a common foundation mat. The internal structure is an assemblage of concentric cylindrical walls and connecting radial walls. The structure has been represented by a model consisting of lumped masses interconnected by beam elements. In addition, compliance functions represented as springs and dashpots attached to the foundation mat incorporate soil-structure interaction by representing stiffness and energy radiation of the underlying soil. The model representing the exterior containment, internal structure and soil stiffness is illustrated in Figure 2 superimposed over a reactor building cross-section. Values for soil spring stiffnesses and dashpot constants for radiation damping were based on Novak [1] for the condition of a rigid base mat resting on elastic half-space and partially embedded in an overlying elastic layer.

Radiation damping in translation is on the order of 55 percent of critical damping. Radiation damping in soil rocking and structure and soil material damping are on the order of 5 to 10 percent. The damping matrix was assumed to be of the following form:

$$[C] = \alpha[M] + \beta[K] + \lceil C_D \rfloor \qquad (1)$$

Mass and stiffness proportional constants, α and β provide 5 to 10 percent of critical damping over the frequency range of interest and correspond to soil and structure material damping and radiation damping in the soil rocking mode. $\lceil C_D \rfloor$ corresponds to the concentrated dashpot values which incorporate the high radiation damping in the soil translational mode.

When placed on a competent rock site with a shear modulus of 8×10^9 Pa (1.2×10^6 psi), this PWR has fundamental frequencies of 4.2 and 5.1 Hz for the containment building and internal structure, respectively. Higher modes have frequencies of 12.9 Hz and higher. These frequencies line up closely with those for which the Melendy Ranch spectral responses are maximized. Thus, from elastic analysis, this structure is being subjected to about 2.5 times as great a response as the SSE response for which it was designed. On softer soil sites, structural responses are shifted to lower frequencies, and the elastic response from the Melendy Ranch record is much reduced. All results presented are for a competent rock site.

With sufficient overturning moment during seismic response, there is a tendency for a portion of the foundation mat to lift off the underlying supporting soil. When only a portion of the foundation mat is in contact with the soil, there is softening of the soil-structure system. This behavior can be simulated by developing a nonlinear moment-rotation relationship for base rocking. Following Ref. [2], the nonlinear base moment, M_B, rotation, Φ_B, relationship shown in Figure 3 was developed where M_u, and Φ_u are the moment and rotation at which uplift is initiated. Similar plots for uplift height and toe pressure were developed. Both showed rapid increases when $|M_B|/M_u$ exceeded 3. Below that level, neither the uplift height or toe pressure were excessive.

3. Inelastic Material Properties

Inelastic behavior of reinforced and prestressed concrete members making up this typical PWR reactor building has been simulated by an elastic beam element with inelastic hinge elements at each end representing flexural stiffness and a short inelastic spring element representing shear stiffness. Beam elements and inelastic flexure and shear springs act in series.

The load-deformation curve used for shear deformations is shown in Figure 4 which is based on the work of Umemura [3, and 4] for shear stiffness and the Takeda [5] model for hysteresis under load reversals. Initially, shear is carried totally by the concrete and the shear stiffness is based upon the concrete shear modulus (slope 1). Once the concrete begins to crack and shear load is picked up by the reinforcement, the stiffness is greatly reduced (slope 2). The "yield" shear strength of the internal structure can be conservatively represented by:

$$v_y = \sqrt{f'_c}\ A'_g\ (10^6)\ /6 \qquad (2)$$

in which v_y in the shear strength (N), f'_c is the concrete unconfined compression strength (MPa), and A'_g is the effective gross concrete area (m^2) which for cylindrical cross-section should be taken as about 80% of the gross concrete area. Eqn. (2) corresponds to a shear stress of $2\sqrt{f'_c}$ in English units and represents a very conservative measure of the strength at which the stiffness of a shear wall reduces. After cracking, the stiffness of the shear wall, K_{S2}, can be conservatively estimated by:

$$K_{S2} = 0.75\rho n K_{S1} \qquad (3)$$

where ρ is the minimum reinforcement ratio in either direction, n is the modular ratio, and K_{S1} is the uncracked shear stiffness. This second slope is followed until the ultimate capacity of concrete plus reinforcing is reached and failure occurs or until load reversal occurs. Unloading stiffness (slope 3), K_{S3}, is substantially reduced due to concrete degradation from the initial stiffness, K_{S1}, and can be represented by:

$$K_{S3} = K_{S1}(\Delta_y/\Delta_u)^{1/2} \qquad (4)$$

where Δ_y is the yield displacement, and Δ_u is the maximum displacement reached. Reloading (slope 5) is on an even softer stiffness toward the point of maximum deformation.

This model is known as a stiffness degrading model. When subjected to a large number of strong ground motion cycles, such as would occur from the 1952 Taft record, each nonlinear cycle results in a substantial increase in the maximum deformation, Δ_u, because of this stiffness degradation. After a number of strong nonlinear cycles, the ultimate capacity is reached and collapse occurs. This model was used as a conservative, yet realistic, model of shear wall behavior to collapse.

A similar model was used for flexural yield hinges. The yield moment, M_y, was assumed to be associated with general yielding of the cross-section. For cylindrical cross-sections, general yielding was taken as corresponding to the steel yield strain being reached in reinforcement at a distance of 0.75D from the compressed edge of the section where D is the outside diameter of the cylinder. The second slope beyond M_y was taken as 3% of the initial slope.

Because of the benefit of compressive confinement provided by the prestressing in the prestressed concrete containment, neither the moment, M_y, or shear, v_y, yield strengths were reached in the containment when subjected to the Melendy Ranch record. Thus, inelastic material properties described above (see Figure 4) were only used for the internal structure.

In addition to inelastic flexural and shear deformations, concentrated rotations at the intersection of the internal structure and base mat due to bond-slip along the reinforcing bars extending into the base mat was considered. Bond-slip rotation, θ_b, is initiated at this interface when a flexural moment, M_b, sufficient to place any of vertical reinforcing bars into tension (i.e., the compressive prestress due to dead load is overcome) is reached. For straight reinforcing bars embedded in the base mat, the yield bond-slip rotation, θ_{by}, corresponding to the flexural yield moment, M_y, can also be estimated for cylindrical cross-section walls. Recall that the yield moment is the moment at which the steel yield strain is reached at a distance of 0.75D from the compressed edge of the cylindrical section. Assume that the length needed to develop the yield strength of the reinforcing bars is $45d_b$ where d_b is the bar diameter. The slip at 0.75D from the compressed edge can be obtained by integrating the steel strain over the development length as follows:

$$\text{slip} = \int_0^{45d_b} \varepsilon_s dx \approx 1/2(f_y/E_s)(45d_b) \qquad (5)$$

$$\text{and} \quad \theta_b y = \frac{\text{slip}}{0.75D-\beta D} = \frac{f_y}{E_s D} \; \frac{45}{2(0.75-\beta)} \qquad (6)$$

where f_y is the steel yield strength, E_s is the steel Young's Modulus, and β is the fraction of the cylinder diameter from the compressed edge to the neutral axis ($\beta \approx 0.1$). Linear interpolation between bond-slip rotation of zero at M_b to θ_{by} at M_y was used.

4. Results

Linear elastic, linear elastic with nonlinear base mat uplift, and inelastic with nonlinear base mat uplift analyses were performed using the Melendy Ranch record as input. Table 1 compares results from these analyses with the linear "yield" and uplift capacities for several key elements. Shear in the internal structure are reported at various heights above the base. In this table, the "yield" base moment corresponds to the moment M_u at which uplift is initiated while the "ultimate" base moment corresponds to the static overturning moment. The "yield" moment capacity for the prestressed concrete containment corresponds to the moment at which tensile cracking is initiated after overcoming the prestress. So long as prestress is retained, shear "yielding" is precluded and shear and moment ultimate capacities are much larger than the Melendy Ranch maximum containment responses.

Linear elastic analysis indicates that the base moment exceeds the moment at which uplift is initiated by a factor of 3.8 and approaches the static overturning moment so that a static overturning analysis using this linear elastic base moment predicts excessively high uplift heights and toe pressures which would result in a foundation failure. The containment remains linear elastic because of the benefit of prestress. The shears within the lower 10 meters of the internal structure exceed the concrete cracking "yield" capacity of the shear walls by as much as a factor of 2.3 and, at 5 meters above the base, the ultimate shear capacity is exceeded which would lead to the prediction of a brittle shear failure for the internal structure. The maximum flexural moement for the internal structure is substantially less than the yield moment but exceeds the moment at which bond-slip is initiated by a factor of 4.4. Based upon a linear elastic analysis, one would wrongfully conclude that the reactor building would suffer a foundation failure and failure of the internal structure if subjected to the Melendy Ranch record.

Elastic uplift analysis results in a substantially reduced base moment and easily tolerable uplift heights and toe pressures. Shear and moment responses throughout the containment and internal structure are reduced to 85 to 90% of the linear elastic results. Shears within the internal structure continue to exceed the concrete cracking "yield" capacity but collapse is no longer predicted by this type of an analysis.

The inelastic uplift analysis shows bond-slip at the internal structure and base mat intersection and shear "yielding" within the lower 6 meters of the internal structure. These local inelastic deformations reduce the elastic responses at other locations throughout the structure. Elastic shears and moments at higher locations in the internal structure are reduced by about a factor of 1.6. Elastic responses in the containment are about 90% while toe pressures and uplift heights are about 95% of the elastic uplift computed responses.

Figure 5 presents the shear force-deformation response for the bottom inelastic portion of the internal structure due to the Melendy Ranch record. One notes only a single cycle of strong inelastic response followed by "pseudo-linear elastic" response with a lesser stiffness and a slight permanent offset of about 0.5 cm. This small offset would not be noticeable nor damaging to the structure nor to components mounted off of it. Minor cracking of the concrete would probably be observable but loss of function would not result from this single inelastic excursion.

Figure 6 compares maximum displacements throughout the reactor building from elastic analysis with uplift versus inelastic analysis. Displacements within the region of inelasticity on the internal structure are increased by up to a factor of 1.3 by inelastic behavior. Displacement of the top of the internal structure is unchanged. Peak accelerations within the region of inelasticity are essentially equal between the two analyses. High within the internal structure, the peak accelerations are reduced by about a factor of 1.6 due to inelastic behavior of lower elevations. Accelerations and displacements on the containment associated with inelastic response of the internal structure ranged from 90 to 100% of those obtained from elastic analysis with uplift.

Floor spectra were generated at several points on the containment and internal structures for all three analyses. Figure 7 compares the floor spectra high on the internal structure (elev. +20m). Floor spectra on the containment from all three analyses were essentially identical ($\pm$10%) indicating that neither base mat uplift nor inelastic response of the internal structure significantly influence these spectra. On the internal structure, the elastic and the elastic with uplift floor spectra were also essentially identical. However, the inelastic floor spectra were substantially reduced. Inelastic spectra on the internal structure were enveloped by spectra from either of the two elastic analyses. The frequency associated with maximum spectral acceleration was lowered by about a factor of 1.4 from 5.1 Hz to 3.6 Hz corresponding to the softening of the force-deformation curve shown in Figure 5. The maximum spectral acceleration was reduced by a factor of 2 by inelastic behavior. Below 3.6 Hz, the elastic and inelastic spectra were essentially identical. Above 5 Hz, the inelastic spectra were a factor of 1.6 to 2.0 less than the elastic spectra. The conclusion is that the local inelasticity of the internal structure helps to protect higher frequency equipment mounted thereon from the Melendy Ranch input.

5. Conclusions

This study investigated the effect of the 0.5g Melendy Ranch Barn record from a magnitude 4.7 earthquake on a PWR reactor building designed for a broad frequency content 0.2g SSE. For frequencies above 4.5 Hz, the Melendy Ranch response spectrum exceeds the design response spectrum by a factor of about 2.5. The fundamental mode of the containment and internal structures were 4.2 and 5.1 Hz and all other modes had frequencies greater than 12.9 Hz. Despite this substantial exceedance, the Melendy Ranch record is not expected to be damaging to this structure. It results in minor base mat uplift of less than 2 mm and acceptable toe pressures on the foundation. Local inelastic shear deformations are expected in the lower portion of the internal structure. However, only a single strong inelastic cycle occurs followed by reduced stiffness "pseudo-elastic" response and a permanent displacement offset of about 0.5 cm. This level of permanent displacement is not expected to be noticeable. This earthquake may result in some minor visible cracking but no degradation of structural capacity for the lower portion of the internal structure. This local inelasticity is expected to generally result in a reduction in structural response and response of equipment attached to the internal structure by a factor of 1.6 to 2.0.

6. Acknowledgement

The study described was performed for Electricité de France, Paris, La Defense, France under the supervision of M. Betbeder.

References

[1] Novak, M., "Vibrations of Embedded Footings", American Society of Civil Engineering National Structural Engineering Meeting, San Francisco, California, April, 1973.

[2] Kennedy, R. P., S. A. Short, D. A. Wesley, T. H. Lee, "Effect of Nonlinear Soil Structure Interaction Due to Base Slab Uplift on the Seismic Response of an HTGR Plant", Nuclear Engineering and Design, Vol. 38, No. 2, Aug., 1976, pp 323-355.

[3] Umemura, H., H. Aoyama, M. Ito, and Y. Hosokawa, "Aseismic Characteristics of R/C Box and Cylinder Walls", Experimental Studies on Reinforced Concrete Members, Vol. 3, Faculty of Engineering, University of Tokyo, December, 1977, pp 49-54.

[4] Umemura, H. H. Aoyama, M. Ito, and Y. Hosokawa, "Tests of Reinforced Concrete Box and Cylinder Walls under Cyclic Loading", Experimental Studies on Reinforced Concrete Members, Vol. 3, Faculty of Engineering, University of Tokyo, December, 1977, pp 32-48.

[5] T. Takeda et al, "Reinforced Concrete Response to Simulated Earthquakes", ASCE Structural Journal, V. 96, No. ST12, December, 1970, pp 2557-2573.

Table 1. Analysis Results

Quantity	Elastic	Elastic Uplift	Inelastic Uplift	Yield	Ultimate
Base Moment ($\times 10^9$ N-m)	9.7	7.3	7.0	2.6	10.4
Uplift Ht. (mm)	63.5	2.2	1.8	—	—
Toe Pressure (MPa)	35.9	3.3	2.9	—	—
Shear at Containment Base ($\times 10^7$ N)	16.1	14.1	13.4	—	—
Moment at Containment Base ($\times 10^9$ N-m)	7.3	6.6	6.2	10.6	—
Shear in Internal Structure ($\times 10^7$ N) Base	17.6	14.9	9.3	7.7	19.6
+5m	17.3	14.6	9.5	7.7	16.7
+8m	15.9	13.5	8.3	13.9	41.2
+12m	13.2	11.5	7.2	17.8	53.6
Moment at Internal Struc. Base ($\times 10^9$ N-m)	3.9	3.5	2.2	7.1*	9.2

1N-m = 8.85 lb-in: 1N = 0.225 lb: 1 mm = 0.04 in: 1MPa = 145 psi

* Bond-Slip $M_b = 0.87 \times 10^9$ N-m

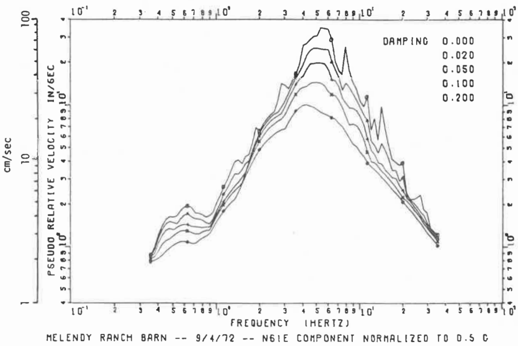

Figure 1. Normalized Melendy Ranch Barn Response Spectrum

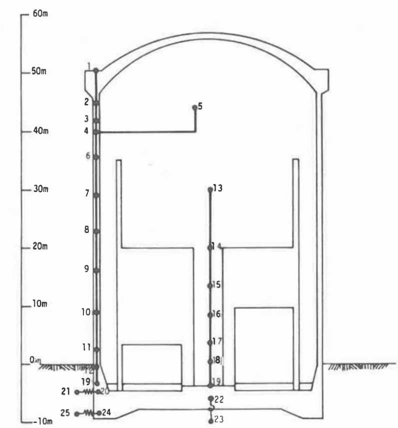

Figure 2. PWR Reactor Building and Analytical Model

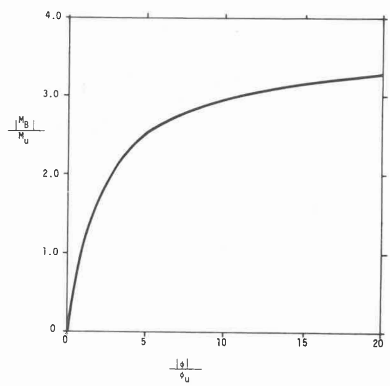

Figure 3. Nonlinear Base Moment-Rotation Relationship

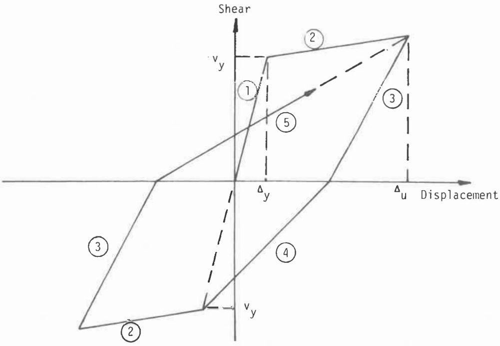

Figure 4. Inelastic Shear Element

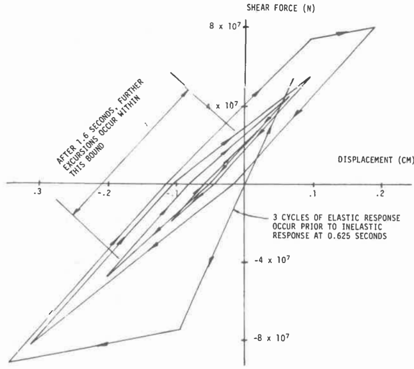

Figure 5. Shear-Displacement Response, Bottom of Internal Structure

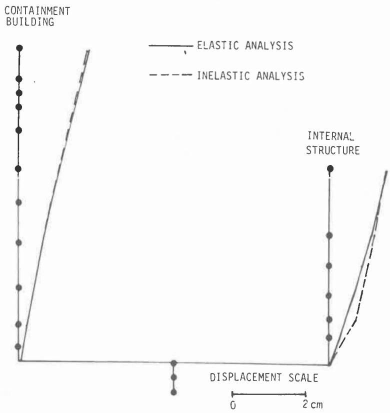

Figure 6. Seismic Response Displacements

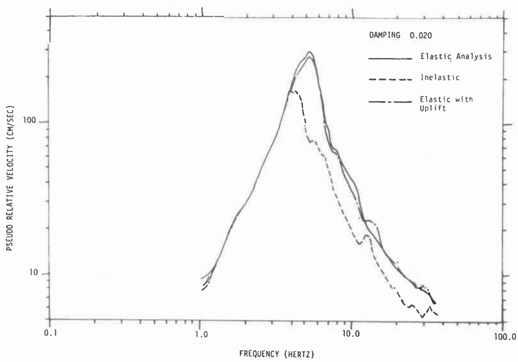

Figure 7. Floor Response Spectra, Internal Structure